CAUCHY – Jurnal Matematika Murni dan Aplikasi
Volume 11 (1) (2026), Pages 1251-1269
p-ISSN: 2086-0382; e-ISSN: 2477-3344

A Mathematical Model of Human-to-Human Transmission of Monkeypox with Reinfection

Eka Widia Rahayu* and Noorma Yulia Megawati

Department of Mathematics, Faculty of Mathematics and Natural Sciences, Universitas Gadjah Mada, Indonesia

Abstract

Monkeypox is a zoonotic disease caused by the monkeypox virus and remains a public health concern due to its potential for sustained human-to-human transmission. This study analyzes the transmission dynamics of monkeypox by developing a deterministic compartmental model that explicitly incorporates reinfection arising from waning immunity. The model is analyzed by deriving the basic reproduction number and determining the disease-free and endemic equilibrium points, whose local and global stability properties are rigorously investigated. A sensitivity analysis is conducted to identify key parameters driving transmission dynamics. Motivated by these results, an optimal control problem is formulated in which vaccination is implemented as a time-dependent control, and the optimal strategy is characterized using Pontryagin's Minimum Principle. Numerical simulations reveal that even low reinfection rates can sustain endemic transmission in the absence of control, while appropriately timed vaccination strategies significantly reduce infection levels and prevent long-term persistence.

Keywords: Mathematical Model; Monkeypox; Reinfection; Optimal Control.

1. Introduction

Infectious diseases continue to pose a serious threat to global public health despite substantial advances in science and technology. Among these, zoonotic diseases warrant particular attention due to their ability to cross species barriers and establish sustained transmission in human populations. In this context, the monkeypox virus (MPXV), the causative agent of monkeypox (mpox), has regained global attention following a recent surge in reported cases accompanied by notable changes in its transmission patterns [1].

Monkeypox was first identified in laboratory monkeys in Denmark in 1958, and the first confirmed human case was reported in the Democratic Republic of the Congo in 1970. For several decades, the disease remained endemic in parts of Central and West Africa, with transmission predominantly driven by animal-to-human spillover. However, since 2022, a substantial increase in human-to-human transmission has been observed in multiple regions worldwide, marking a critical shift in the epidemiological dynamics of mpox [1]. Human-to-human transmission has therefore become a major public health concern, as the virus can spread through close contact with skin lesions, bodily fluids, respiratory droplets, or contaminated objects [2].

*Corresponding author. E-mail: ekawidiarahayu@mail.ugm.ac.id

Submitted: January 05, 2026 Reviewed: January 18, 2026 Accepted: May 21, 2026
DOI: https://doi.org/10.18860/cauchy.v11i1.40140

Unlike smallpox, which has humans as its sole natural host, mpox is sustained by multiple animal reservoirs, including rodents and primates, and exhibits the potential for reverse zoonosis, allowing transmission from humans back to animals [2]. This ecological complexity increases the likelihood of long-term viral persistence and complicates eradication efforts. Moreover, accumulating epidemiological evidence suggests that immunity acquired through natural infection or vaccination against MPXV may not be lifelong, thereby opening the possibility of reinfection after a certain period.

Documented cases of mpox reinfection [3], although still relatively rare, indicate that post-infection immunity does not necessarily confer permanent protection. Preliminary clinical and epidemiological studies suggest that reinfection may arise due to waning immune responses or viral mutations that alter antigenic properties. From an epidemiological perspective, reinfection events are unlikely to be the primary drivers of short-term outbreaks but may play a crucial role in prolonging transmission chains and facilitating the transition of mpox toward recurrent endemicity rather than complete elimination. Consequently, neglecting reinfection mechanisms in transmission models may lead to overly optimistic predictions regarding disease control and eradication.

The impermanent nature of immunity also implies that effective mpox control depends not only on vaccine availability but critically on how, when, and to what extent vaccination is implemented within the population. In practice, vaccination policies are inherently dynamic, shaped by vaccine supply constraints, prioritization of high-risk groups, and the evolving severity of outbreaks. Nevertheless, many existing mathematical models of mpox transmission assume permanent immunity following recovery or vaccination and incorporate control interventions as static parameters or fixed compartments [4]. Such formulations may inadequately capture the adaptive and time-dependent nature of real-world public health decision-making, particularly in the presence of waning immunity and reinfection.

In Indonesia and several other countries, recent declines in mpox cases have been largely attributed to non-pharmaceutical interventions, including contact tracing, isolation, and public education aimed at behavioral change [2]. Despite these efforts, continued human-to-human transmission and the absence of widespread herd immunity indicate that the risk of resurgence remains substantial. Given the potential for sustained transmission driven by reinfection, a deeper understanding of the underlying transmission dynamics in human populations is essential. Mathematical modeling provides a powerful framework for identifying conditions that lead to repeated outbreaks, assessing the potential for endemic persistence, and formulating evidence-based intervention strategies.

Several recent mathematical models have contributed substantially to understanding mpox transmission dynamics. Peter et al. [5] developed a compartmental model incorporating multiple intervention strategies and demonstrated that isolation and treatment are effective in reducing transmission, yet their model assumes permanent immunity following recovery and treats all control interventions as time-invariant parameters. Similarly, Ahmad et al. [4] extended the human-to-human mpox framework by incorporating post-exposure vaccination as a fixed compartmental transition, providing valuable insights into the role of vaccination coverage; however, the possibility of reinfection due to waning immunity was not considered, and vaccination was not formulated as a time-dependent adaptive strategy. Usman and Isa Adamu [6] also examined mpox transmission with vaccination and treatment interventions, yet their formulation likewise assumes lifelong post-infection immunity and does not account for the dynamically adaptive nature of real-world vaccination deployment. More broadly, the majority of existing mpox models adopt one of two simplifying assumptions that limit their epidemiological realism: either immunity is assumed permanent, precluding the possibility of reinfection, or control interventions are incorporated as static parameters rather than dynamic decision variables. The present study addresses both limitations simultaneously. Specifically, we develop a deterministic $SEAIHR$ compartmental model that explicitly incorporates waning

immunity and reinfection as a feedback mechanism from the recovered to the susceptible class, and formulates vaccination as a time-dependent optimal control variable characterized via Pontryagin's Minimum Principle. This dual novelty allows the model to capture the potential for endemic persistence driven by reinfection while simultaneously providing an analytically rigorous and adaptive framework for designing cost-effective vaccination strategies.

2. Methods

In this study, a deterministic compartmental model is proposed to describe the transmission dynamics of mpox in a human population under the effects of reinfection and vaccination. The population is partitioned into six mutually exclusive compartments: susceptible individuals $S(t)$, exposed individuals $E(t)$, asymptomatic infected individuals $A(t)$, symptomatic infected individuals $I(t)$, isolated individuals $H(t)$, and recovered individuals $R(t)$. The total population size at time t is given by

$$N(t) = S(t) + E(t) + A(t) + I(t) + H(t) + R(t).$$

The model assumes that transmission occurs exclusively through human-to-human contact and is driven by interactions between susceptible individuals and symptomatic infected individuals. This modeling choice reflects the dominant transmission mechanism observed in recent mpox outbreaks, where sustained spread has primarily been associated with close physical contact involving symptomatic cases. Asymptomatic infected individuals are therefore assumed to have negligible transmissibility, allowing the force of infection to be represented as a function of the symptomatic compartment alone and ensuring analytical tractability of the model. The force of infection is modeled using the mass-action incidence term βIS, which assumes that the rate of new infections is proportional to both the number of susceptible individuals and the number of symptomatic infected individuals. This formulation is appropriate under the assumption of homogeneous mixing in a population where contact rates increase with population density, reflecting localized transmission dynamics characteristic of community-level mpox outbreaks. Under this formulation, the parameter β represents the effective transmission rate per susceptible–infectious pair, with units of inverse population per unit time. This contrasts with the frequency-dependent formulation $\frac{\beta IS}{N}$, in which the contact rate is assumed independent of population size — an assumption more appropriate for spatially structured or large heterogeneous populations. The choice of mass-action incidence is consistent with several existing mpox modeling studies operating at the community level, including Peter et al. [5] and Ahmad et al. [4].

Following exposure, individuals enter the incubation class E before progressing, at rate α, either to the asymptomatic infected class A with proportion $(1-p)$ or directly to the symptomatic infected class I with proportion p. Individuals in the asymptomatic class may subsequently progress to symptomatic infection at rate σ, or recover without clinical manifestation at rate ψ, depending on immune response. Symptomatic infected individuals may recover naturally at rate τ or, in cases of severe infection, be transferred to the isolation compartment H at rate ϕ, where they receive medical treatment or clinical monitoring and are assumed to have no further contact with the susceptible population. Recovery from the isolated class occurs at rate γ. Disease-induced mortality is assumed to occur only among symptomatic and isolated individuals, at a constant rate δ, reflecting the observation that clinical complications and fatalities in mpox are predominantly associated with the symptomatic stage of infection..

Recovered individuals are assumed to acquire temporary immunity. To account for waning immunity and reported cases of reinfection [3], recovered individuals may return to the susceptible class at a constant rate ν. This mechanism introduces a feedback loop from the recovered to the susceptible compartment, which plays a crucial role in shaping the long-term dynamics of the system and allows for the possibility of disease persistence and endemic equilibrium states. When $\nu \to 0$, the model reduces to the classical framework with permanent post-infection immunity. Table 1 represent the variables and parameters used in model formation.

Table 1: Interpretation of the state variables and parameters used in the model

Variable	Description
β	Effective contact rate between susceptible individuals and symptomatic infected individuals.
α	Rate at which exposed individuals progress to the infectious stage after the incubation period.
p	Proportion of exposed individuals who develop symptomatic infection upon completing the incubation period.
σ	Rate at which asymptomatic infected individuals progress to symptomatic infection.
ψ	Rate at which asymptomatic infected individuals recover without developing clinical symptoms.
ϕ	Rate at which symptomatic infected individuals are detected and transferred to the isolated class.
τ	Rate at which symptomatic infected individuals recover without entering formal isolation.
γ	Rate at which isolated individuals recover.
ν	Rate at which recovered individuals lose immunity and return to the susceptible class.

A schematic diagram of the mpox transmission model with reinfection is illustrated in Fig. 1.

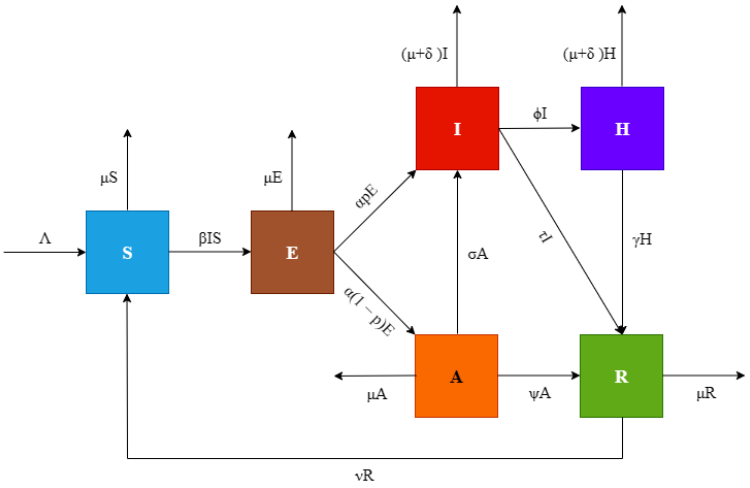

Fig. 1: Schematic diagram of the model

Based on the schematic diagram, the mathematical model for mpox transmission is formulated as follows.

$$\begin{aligned}
\frac{dS}{dt} &= \Lambda + \nu R - \beta IS - \mu S \\
\frac{dE}{dt} &= \beta IS - (\mu + \alpha)E \\
\frac{dA}{dt} &= \alpha(1-p)E - (\sigma + \psi + \mu)A \\
\frac{dI}{dt} &= \alpha pE + \sigma A - (\mu + \delta + \phi + \tau)I \\
\frac{dH}{dt} &= \phi I - (\mu + \delta + \gamma)H \\
\frac{dR}{dt} &= \psi A + \tau I + \gamma H - (\mu + \nu)R,
\end{aligned} \tag{1}$$

where the initial condition is given by $S(0) > 0, E(0) \geq 0, A(0) \geq 0, I \geq 0, H \geq 0$, and $R(0) \geq 0$.

3. Results and Discussion

This section presents the analytical and numerical results derived from the proposed mathematical model for monkeypox transmission. The analytical study encompasses the formulation of the

mathematical model, the derivation of the basic reproduction number, and the determination of both the disease-free and endemic equilibrium points. Stability analyses of these equilibrium points, along with a sensitivity analysis of the basic reproduction number, are subsequently carried out. An optimal control problem governing monkeypox transmission is further formulated and analyzed. Numerical simulations are then performed to corroborate and complement the analytical findings obtained from the model.

3.1. Analytical Results

The nonnegativity and boundedness of solutions of the proposed model can be established using standard results from dynamical systems theory, as described in [7], [8], and [9]. The following theorem demonstrates that the feasible region of system (1) is a positively invariant set. This feasible region is defined as follows.

$$\Omega = \left\{ (S, E, A, I, H, R) \in \mathbb{R}_+^6 : 0 \leq S + E + A + I + H + R \leq \frac{\Lambda}{\mu} \right\} \tag{2}$$

Theorem 1. *The set Ω is a bounded positive invariant set of system (1) with initial conditions $S(0) > 0, E(0) \geq 0, A(0) \geq 0, I(0) \geq 0, H(0) \geq 0$, and $R(0) \geq 0$.*

Proof. Note that $N = S + E + A + I + H + R$ denotes the total population size at time t. Differentiating $N(t)$ with respect to time yields

$$\begin{aligned} \frac{dN}{dt} &= \frac{dS}{dt} + \frac{dE}{dt} + \frac{dA}{dt} + \frac{dI}{dt} + \frac{dH}{dt} + \frac{dR}{dt} \\ &= \Lambda - \mu N - \delta I - \delta H \\ &\leq \Lambda - \mu N. \end{aligned}$$

Consider

$$\frac{dX}{dt} = \Lambda - \mu X, \tag{3}$$

where $X(0) = N(0)$. Solving Eq. (3) using the integrating factor method and by the Comparison Theorem yields,

$$0 \leq N(t) \leq \frac{\Lambda}{\mu} + \left(N(0) - \frac{\Lambda}{\mu} \right) e^{-\mu t}, \tag{4}$$

Next, we show that the set Ω is a positively invariant set. Let any initial condition satisfy $N(0) \in \Omega$, that is $N(0) \leq \frac{\Lambda}{\mu}$. Then, from Eq. (4), for all $t \geq 0$,

$$\begin{aligned} \lim_{t\to\infty} (S + E + A + I + H + R) &\leq \lim_{t\to\infty} N(t) \\ &= \lim_{t\to\infty} \frac{\Lambda}{\mu} + \left(N(0) - \frac{\Lambda}{\mu} \right) e^{-\mu t} \\ &= \frac{\Lambda}{\mu}. \end{aligned} \tag{5}$$

Therefore, $0 \leq N(t) \leq \frac{\Lambda}{\mu}$, and the set Ω is a positively invariant and bounded set. □

3.1.1. Disease-free equilibrium points

We next consider the disease-free equilibrium of system (1), corresponding to the absence of infection. The mpox-free equilibrium, denoted by $\mathcal{E}_0$ is given by

$$\mathcal{E}_0 = (S^0, E^0, A^0, I^0, H^0, R^0) = \left(\frac{\Lambda}{\mu}, 0, 0, 0, 0, 0\right). \tag{6}$$

3.1.2. Basic reproduction number

Next, we determine the basic reproduction number for system (1) using the next-generation matrix method [10–12]. The basic reproduction number, denoted by $\mathcal{R}_0$, represents the average number of secondary infections generated by a single infectious individual in a wholly susceptible population. Following the standard framework, $\mathcal{R}_0$ is defined as the spectral radius of the next-generation matrix, given by

$$\mathcal{R}_0 = \rho\left(FV^{-1}\right).$$

To compute this quantity, we construct the vector F_i, which represents the rate of appearance of new infections in each infected compartment, and the vector V_i, which accounts for all other transition processes, including progression, recovery, and removal. For system (1), these vectors are given by

$$\boldsymbol{F_i} = \begin{bmatrix} \beta IS \\ 0 \\ 0 \\ 0 \end{bmatrix}, \quad \boldsymbol{V_i} = \begin{bmatrix} (\mu+\alpha)E \\ (\sigma+\psi+\mu)A - \alpha(1-p)E \\ (\mu+\delta+\phi+\tau)I - \alpha pE - \sigma A \\ (\mu+\delta+\gamma)H - \phi I \end{bmatrix}.$$

Linearizing $\boldsymbol{F_i}$ and $\boldsymbol{V_i}$ at the disease-free equilibrium point yields the Jacobian matrices $\boldsymbol{F}$ and $\boldsymbol{V}$, respectively, given by

$$\boldsymbol{F} = \begin{bmatrix} 0 & 0 & \beta S^0 & 0 \\ 0 & 0 & 0 & 0 \\ 0 & 0 & 0 & 0 \\ 0 & 0 & 0 & 0 \end{bmatrix}, \tag{7}$$

where $S^0 = \dfrac{\Lambda}{\mu}$, and

$$\boldsymbol{V} = \begin{bmatrix} \alpha+\mu & 0 & 0 & 0 \\ -\alpha(1-p) & \sigma+\psi+\mu & 0 & 0 \\ -\alpha p & -\sigma & \mu+\delta+\phi+\tau & 0 \\ 0 & 0 & -\phi & \mu+\delta+\gamma \end{bmatrix}. \tag{8}$$

Consequently, the basic reproduction number is obtained as

$$\begin{aligned} \mathcal{R}_0 &= \rho\left(FV^{-1}\right) \\ &= \frac{\alpha\beta\Lambda[\sigma(1-p) + (\sigma+\psi+\mu)p]}{\mu(\alpha+\mu)(\sigma+\psi+\mu)(\mu+\delta+\phi+\tau)}. \end{aligned}$$

Biologically, the basic reproduction number $\mathcal{R}_0$ represents the expected number of secondary mpox cases generated by a single infectious individual in a fully susceptible population. Its expression reflects three key mechanisms governing transmission: the *contact factor*, determined by the transmission rate β; the *progression factor*, characterized by the rates α, p, and σ describing the transition from exposure to infectious states; and the *infection duration factor*, given by the inverse of the combined recovery, isolation, and removal rates $(\mu+\delta+\phi+\tau)^{-1}$. While $\mathcal{R}_0$ does not explicitly depend on the reinfection rate ν, since it is defined at the disease-free equilibrium, reinfection plays a crucial role in the long-term dynamics by replenishing the susceptible population through waning immunity and thereby promoting endemic persistence beyond the initial invasion threshold.

3.1.3. Endemic equilibrium points

The endemic equilibrium corresponds to a steady state at which the disease persists in the population. The following theorem characterizes the existence of the endemic equilibrium point.

Theorem 2. *If $\mathcal{R}_0 > 1$ and $(k_1 - \nu L) > 0$, then system (1) admits a unique endemic equilibrium point*

$$\mathcal{E}_1 = (S^*, E^*, A^*, I^*, H^*, R^*),$$

with components given by

$$\begin{aligned} S^* &= \frac{k_1 k_2 k_3}{\alpha\beta\left[pk_2 + (1-p)\sigma\right]}, \quad E^* = \frac{\Lambda\left(1 - \frac{1}{\mathcal{R}_0}\right)}{k_1 - \nu L}, \quad A^* = \left(\frac{\alpha(1-p)}{k_2}\right) E^*, \\ I^* &= \left(\frac{\alpha p k_2 + \alpha(1-p)\sigma}{k_2 k_3}\right) E^*, \quad H^* = \frac{\phi\left[\alpha p k_2 + \alpha(1-p)\sigma\right]}{k_2 k_3 k_4} E^*, \quad R^* = LE^*, \end{aligned} \tag{9}$$

where

$$\begin{aligned} k_1 &= \mu + \alpha, \quad k_2 = \mu + \sigma + \psi, \quad k_3 = \mu + \delta + \phi + \tau, \quad k_4 = \mu + \delta + \gamma, \\ L &= \frac{\psi k_3 k_4[\alpha(1-p)] + \tau k_4[\alpha p k_2 + \alpha(1-p)\sigma] + \gamma\phi[\alpha p k_2 + \alpha(1-p)\sigma]}{k_2 k_3 k_4(\mu + \nu)}. \end{aligned}$$

Proof. The endemic equilibrium point of System (1) is obtained by solving the following system of nonlinear algebraic equations:

$$0 = \Lambda + \nu R^* - \beta I^* S^* - \mu S^*, \tag{10}$$
$$0 = \beta I^* S^* - (\mu + \alpha) E^*, \tag{11}$$
$$0 = \alpha(1-p) E^* - (\sigma + \psi + \mu) A^*, \tag{12}$$
$$0 = \alpha p E^* + \sigma A^* - (\mu + \delta + \phi + \tau) I^*, \tag{13}$$
$$0 = \phi I^* - (\mu + \delta + \gamma) H^*, \tag{14}$$
$$0 = \psi A^* + \tau I^* + \gamma H^* - (\mu + \nu) R^*. \tag{15}$$

From Eq. (12) yields

$$A^* = \frac{\alpha(1-p)}{k_2} E^*.$$

From Eq. (13), we obtain

$$I^* = \frac{\alpha p k_2 + \alpha(1-p)\sigma}{k_2 k_3} E^*.$$

Similarly, from Eq. (14) gives

$$H^* = \frac{\phi[\alpha p k_2 + \alpha(1-p)\sigma]}{k_2 k_3 k_4} E^*.$$

From Eq. (11), we obtain

$$S^* = \frac{k_1 k_2 k_3}{\alpha\beta[pk_2 + (1-p)\sigma]}.$$

Next, from in Eq. (15) yields

$$R^* = LE^*.$$

Finally, substituting these expressions into Eq. (10) gives

$$\Lambda\left(1 - \frac{1}{\mathcal{R}_0}\right) = (k_1 - \nu L) E^*,$$

which implies

$$E^* = \frac{\Lambda\left(1 - \frac{1}{\mathcal{R}_0}\right)}{k_1 - \nu L}.$$

Hence, if $\mathcal{R}_0 > 1$ and $(k_1 - \nu L) > 0$, then $E^* > 0$, and the endemic equilibrium point exists uniquely. □

The condition $(k_1 - \nu L) > 0$ ensures that reinfection does not dominate demographic turnover and disease progression, thereby preserving the existence of a biologically meaningful endemic equilibrium. When $\nu \to 0$, the model reduces to the classical mpox framework with permanent immunity, and the endemic equilibrium coincides with that of standard models without reinfection.

3.1.4. Local stability of disease-free equilibrium points

Theorem 3. *If $\mathcal{R}_0 < 1$, then the disease-free equilibrium point in Eq. (16) is locally-asymtotically stable.*

Proof. We form the Jacobian matrix of system (1) at the disease-free equilibrium point as follows.

$$\boldsymbol{\mathcal{D}}\mathbf{f}(\boldsymbol{\mathcal{E}_0}) = \begin{bmatrix} -\mu & 0 & 0 & -\beta S^0 & 0 & \nu \\ 0 & -k_1 & 0 & \beta S^0 & 0 & 0 \\ 0 & \alpha(1-p) & -k_2 & 0 & 0 & 0 \\ 0 & \alpha p & \sigma & -k_3 & 0 & 0 \\ 0 & 0 & 0 & \phi & -k_4 & 0 \\ 0 & 0 & \psi & \tau & \gamma & -(\mu+\nu) \end{bmatrix}$$

with

$$k_1 = \mu + \alpha, k_2 = \mu + \sigma + \psi, k_3 = \mu + \delta + \phi + \tau, k_4 = \mu + \delta + \gamma.$$

Then, the eigenvalue of the matrix $\boldsymbol{\mathcal{D}f(\mathcal{E}_0)}$ will be determined as follows.

$$|\lambda \boldsymbol{I} - \boldsymbol{\mathcal{D}}\mathbf{f}(\boldsymbol{\mathcal{E}_0})| = 0$$

$$\begin{vmatrix} \lambda+\mu & 0 & 0 & \beta S^0 & 0 & -\nu \\ 0 & \lambda+k_1 & 0 & -\beta S^0 & 0 & 0 \\ 0 & -\alpha(1-p) & \lambda+k_2 & 0 & 0 & 0 \\ 0 & -\alpha p & -\sigma & \lambda+k_3 & 0 & 0 \\ 0 & 0 & 0 & -\phi & \lambda+k_4 & 0 \\ 0 & 0 & -\psi & -\tau & -\gamma & \lambda+(\mu+\nu) \end{vmatrix} = 0.$$

Solving the characteristic equation of the Jacobian matrix yields the following eigenvalues:

$$\begin{aligned} \lambda_1 &= -\mu < 0 \\ \lambda_2 &= -(\mu+\alpha) < 0 \\ \lambda_3 &= -(\sigma+\psi+\mu) < 0 \\ \lambda_4 &= -(\mu+\delta+\gamma) < 0 \\ \lambda_5 &= -(\mu+\nu) < 0 \\ \lambda_6 &= \frac{\beta S^0\alpha(1-p)\sigma+\beta S^0(\sigma+\psi+\mu)\alpha p-(\mu+\alpha)(\sigma+\psi+\mu+\tau)(\mu+\delta+\phi+\tau)}{(\mu+\alpha)(\sigma+\delta+\gamma)} \\ &= \frac{\alpha\beta S^0[(1-p)\sigma+(\sigma+\psi+\mu)p]-(\mu+\alpha)(\sigma+\psi+\mu+\tau)(\mu+\delta+\phi+\tau)}{(\mu+\alpha)(\sigma+\delta+\gamma)} \\ &= \frac{\alpha\beta\frac{\Lambda}{\mu}[(1-p)\sigma+(\sigma+\psi+\mu)p]-(\mu+\alpha)(\sigma+\psi+\mu+\tau)(\mu+\delta+\phi+\tau)}{(\mu+\alpha)(\sigma+\delta+\gamma)}. \end{aligned}$$

Eigenvalue λ_6 is negative if and only if

$$\alpha\beta\frac{\Lambda}{\mu}[\sigma(1-p)+(\sigma+\psi+\mu)p]-(\alpha+\mu)(\sigma+\psi+\mu)(\mu+\delta+\phi+\tau)<0.$$

which implied $\mathcal{R}_0<1$. Therefore, if $\mathcal{R}_0<1$ the disease-free equilibrium point

$$\mathcal{E}_0=(S^0,E^0,A^0,I^0,H^0,R^0)=\left(\frac{\Lambda}{\mu},0,0,0,0,0\right). \tag{16}$$

is locally-asymptotically stable. □

3.1.5. Global stability of disease-free equilibrium points

The global behavior of the model is analyzed by investigating the global stability of its equilibrium points through Lyapunov's direct method, following the theoretical foundations in [13, 14].

Theorem 4. *If $\mathcal{R}_0<1$, then the disease-free equilibrium point in Eq. (16) is globally-asymtotically stable.*

Proof. Consider the Lyapunov function $Y:\mathbb{R}^3_+\to\mathbb{R}$ defined by

$$Y(E,A,I)=d_1E+d_2A+d_3I, \tag{17}$$

where $d_1,d_2,d_3>0$ are given by

$$\begin{aligned}d_1&=\frac{\alpha[\sigma(1-p)+(\sigma+\psi+\mu)p]}{(\alpha+\mu)(\sigma+\psi+\mu)(\mu+\delta+\phi+\tau)},\\ d_2&=\frac{\sigma}{(\sigma+\psi+\mu)(\mu+\delta+\phi+\tau)},\\ d_3&=\frac{1}{\mu+\delta+\phi+\tau}.\end{aligned}$$

Let $k_1=\alpha+\mu$, $k_2=\sigma+\psi+\mu$, and $k_3=\mu+\delta+\phi+\tau$. Differentiating Y along solutions of System (1) yields

$$\begin{aligned}\dot{Y}&=d_1\dot{E}+d_2\dot{A}+d_3\dot{I}\\ &=d_1[\beta IS-k_1E]+d_2[\alpha(1-p)E-k_2A]+d_3[\alpha pE+\sigma A-k_3I].\end{aligned}$$

Substituting the coefficients d_1,d_2,d_3 and simplifying, we obtain

$$\dot{Y}=\frac{\alpha\beta\Lambda[\sigma(1-p)+k_2p]}{\mu k_1k_2k_3}I-I=(\mathcal{R}_0-1)I.$$

Hence, $\dot{Y}\le 0$ for all $(E,A,I)\in\mathbb{R}^3_+$ whenever $\mathcal{R}_0<1$, with equality if and only if $I=0$. Define the invariant set as

$$\mathcal{T}=\{(E,A,I)\in\mathbb{R}^3_+:\dot{Y}=0\}=\{(E,A,I)\in\mathbb{R}^3_+:E=A=I=0\}.$$

On $\mathcal{T}$, System (1) reduces to

$$\begin{aligned}\frac{dS}{dt}&=\Lambda+\nu R-\mu S,\\ \frac{dH}{dt}&=-(\mu+\delta+\gamma)H,\\ \frac{dR}{dt}&=\gamma H-(\mu+\nu)R.\end{aligned} \tag{18}$$

The solutions satisfy

$$H(t) \to 0, \quad R(t) \to 0, \quad S(t) \to \frac{\Lambda}{\mu} \quad \text{as } t \to \infty.$$

Therefore,

$$(S(t), E(t), A(t), I(t), H(t), R(t)) \longrightarrow \left(\frac{\Lambda}{\mu}, 0, 0, 0, 0, 0\right) = \mathcal{E}_0.$$

By LaSalle's Invariance Principle, the disease-free equilibrium point $\mathcal{E}_0$ is globally asymptotically stable whenever $\mathcal{R}_0 < 1$. □

3.1.6. Global stability of endemic equilibrium points

Proposition 1. *Assume that $\mathcal{R}_0 > 1$ and $(k_1 - \nu L) > 0$. Under the sufficient conditions $S \geq S^*$, $E \geq E^*$, $A \geq A^*$, $I \geq I^*$, $H \geq H^*$, and $R \geq R^*$, that guarantee monotonicity in the feasible region, the endemic equilibrium point $\mathcal{E}_1$ is conditionally globally asymptotically stable.*

Proof. Assume that $\mathcal{R}_0 > 1$ and $(k_1 - \nu\eta) > 0$, so that the endemic equilibrium $\mathcal{E}_1 = (S^*, E^*, A^*, I^*, H^*, R^*)$ exists. Consider the Lyapunov function $Y : \mathbb{R}^6_+ \to \mathbb{R}$ defined by

$$Y(S, E, A, I, H, R) = \frac{1}{2}\Big[(S-S^*)+(E-E^*)+(A-A^*)+(I-I^*)+(H-H^*)+(R-R^*)\Big]^2. \quad (19)$$

Clearly, $Y \geq 0$ for all $(S, E, A, I, H, R) \in \mathbb{R}^6_+$ and $Y = 0$ if and only if $(S, E, A, I, H, R) = \mathcal{E}_1$. Let $N = S + E + A + I + H + R$. Since $\mathcal{E}_1$ satisfies system (1), the equilibrium identity

$$\Lambda = \mu(S^* + E^* + A^* + I^* + H^* + R^*) + \delta(I^* + H^*) \quad (20)$$

holds. Differentiating Y along the trajectories of system (1) yields

$$\dot{Y} = \Big[(S - S^*) + (E - E^*) + (A - A^*) + (I - I^*) + (H - H^*) + (R - R^*)\Big]\big(\Lambda - \mu N - \delta I - \delta H\big).$$

Using Eq. (20) and rearranging terms, we obtain

$$\begin{aligned}\dot{Y} = &-\mu\Big[(S - S^*) + (E - E^*) + (A - A^*) + (I - I^*) + (H - H^*) + (R - R^*)\Big]^2 \\ &- \delta(I - I^*)^2 - \delta(H - H^*)^2 \\ &- \delta(I - I^*) \sum_{X \in \{S,E,A,H,R\}} (X - X^*) - \delta(H - H^*) \sum_{X \in \{S,E,A,I,R\}} (X - X^*).\end{aligned}$$

Now impose the sufficient conditions $S \geq S^*$, $E \geq E^*$, $A \geq A^*$, $I \geq I^*$, $H \geq H^*$, and $R \geq R^*$. Under these conditions, we have $(X - X^*) \geq 0$ for all relevant state variables, and hence each product term $-(I - I^*)\sum(\cdot)$ and $-(H - H^*)\sum(\cdot)$ is non-positive. Therefore, $\dot{Y} \leq 0$, with $\dot{Y} = 0$ if and only if

$$S = S^*, \quad E = E^*, \quad A = A^*, \quad I = I^*, \quad H = H^*, \quad R = R^*,$$

that is, if and only if $(S, E, A, I, H, R) = \mathcal{E}_1$.
Let

$$\mathcal{T} = \{(S, E, A, I, H, R) \in \mathbb{R}^6_+ : \dot{Y} = 0\}.$$

Then the largest invariant set contained in $\mathcal{T}$ is the singleton $\{\mathcal{E}_1\}$. By LaSalle's Invariance Principle, the equilibrium point $\mathcal{E}_1$ is asymptotically stable under the sufficient conditions $S \geq S^*$, $E \geq E^*$, $A \geq A^*$, $I \geq I^*$, $H \geq H^*$, and $R \geq R^*$. □

3.1.7. Sensitivity analysis

To identify the most influential parameters driving mpox transmission, a sensitivity analysis of the basic reproduction number $\mathcal{R}_0$ is performed using the normalized forward sensitivity index method [15]. The basic reproduction number is given by

$$\mathcal{R}_0 = \frac{\Lambda\alpha\beta[\sigma(1-p)+(\sigma+\psi+\mu)p]}{\mu(\alpha+\mu)(\sigma+\psi+\mu)(\mu+\delta+\phi+\tau)}.$$

The sensitivity index of $\mathcal{R}_0$ with respect to a parameter x is defined as

$$I_x^{\mathcal{R}_0} = \frac{\partial \mathcal{R}_0}{\partial x}\frac{x}{\mathcal{R}_0}.$$

Analytical computation shows that $\mathcal{R}_0$ is positively sensitive to the parameters

$$\beta,\ \Lambda,\ \alpha,\ \sigma,\ \text{and } p,$$

and negatively sensitive to

$$\psi,\ \delta,\ \phi,\ \text{and } \tau.$$

Positive sensitivity indices indicate that increases in transmission-related and progression parameters enhance disease spread, while negative sensitivity indices imply that increasing recovery, isolation, and treatment rates reduces $\mathcal{R}_0$. These results provide direct guidance for the optimal control strategy formulated in this study: parameters with negative sensitivity indices correspond to control mechanisms that should be strengthened. In particular, increasing the isolation rate ϕ and treatment rate τ, together with effective vaccination that reduces the susceptible population, contributes significantly to lowering $\mathcal{R}_0$ and suppressing transmission. Conversely, the strong positive sensitivity of $\mathcal{R}_0$ to β highlights the importance of early vaccination and behavioral interventions aimed at reducing effective contact rates. The normalized sensitivity indices of $\mathcal{R}_0$ are summarized in Table 2.

Table 2: Summary of normalized sensitivity indices of $\mathcal{R}_0$

Parameter	Sensitivity Index	Sign	Interpretation and Control Implication
β	$+1$	$+$	Strongly increases transmission; reducing effective contact through vaccination and behavioral interventions is crucial.
Λ	$+1$	$+$	Higher recruitment enlarges susceptible pool; highlights importance of sustained control efforts.
α	$\frac{\mu}{\alpha+\mu}$	$+$	Faster progression from exposed to infected increases spread.
σ	>0	$+$	Accelerates transition to infectious class, enhancing transmission.
p	>0	$+$	Higher probability of symptomatic infection increases transmission potential.
ψ	<0	$-$	Faster recovery of asymptomatic individuals reduces transmission.
δ	<0	$-$	Disease-induced removal decreases transmission, though not a control target.
ϕ	<0	$-$	Isolation of symptomatic cases significantly suppresses transmission.
τ	<0	$-$	Treatment of symptomatic individuals lowers infectious duration.

The reinfection parameter ν does not explicitly appear in the analytical expression of the basic reproduction number $\mathcal{R}_0$. However, ν strongly influences the long-term endemic dynamics

by replenishing the susceptible population through waning immunity, thereby promoting endemic persistence despite not affecting the initial invasion threshold.

The sensitivity analysis supports the optimal control results by identifying recovery, isolation, treatment, and vaccination-related mechanisms as the most effective levers for controlling mpox outbreaks.

3.1.8. Optimal control problem

The optimal control problem aims to determine an effective prevention and intervention strategy to minimize mpox transmission while accounting for the associated medical and non-medical costs. Specifically, the objective is to reduce the infected subpopulations, namely the exposed class (E), asymptomatic infected class (A), and symptomatic infected class (I), which were identified in the sensitivity analysis as key contributors to the basic reproduction number $\mathcal{R}_0$.

Motivated by the sensitivity results, which show that $\mathcal{R}_0$ is strongly positively sensitive to the transmission rate β and negatively sensitive to recovery, isolation, and treatment parameters, vaccination is introduced as the primary time-dependent control. The control variable $u(t)$ represents the vaccination effort applied to the susceptible population. To reflect imperfect vaccine protection, the parameter $\epsilon \in (0, 1]$ denotes vaccine efficacy, representing the fraction of vaccinated individuals who successfully acquire immunity.

Under this control strategy, the controlled mpox transmission model is given by

$$\begin{aligned}
\frac{dS}{dt} &= \Lambda - \beta IS - \mu S + \nu R - \epsilon uS \\
\frac{dE}{dt} &= \beta IS - (\mu + \alpha)E \\
\frac{dA}{dt} &= \alpha(1-p)E - (\sigma + \psi + \mu)A \\
\frac{dI}{dt} &= \alpha pE + \sigma A - (\mu + \delta + \phi + \tau)I \\
\frac{dH}{dt} &= \phi I - (\mu + \delta + \gamma)H \\
\frac{dR}{dt} &= \psi A + \tau I + \gamma H - (\mu + \nu)R + \epsilon uS.
\end{aligned} \tag{21}$$

The initial conditions satisfy

$$S(0) > 0, \quad E(0), A(0), I(0), H(0), R(0) \geq 0.$$

The corresponding objective functional is defined as

$$J(u) = \int_{t_0}^{t_f} \left(w_1 E(t) + w_2 A(t) + w_3 I(t) + \frac{1}{2} w_4 u^2(t) \right) dt,$$

where w_1, w_2, and w_3 represent the relative importance of reducing each infected compartment, while w_4 penalizes excessive vaccination effort. This formulation directly reflects the sensitivity analysis: greater emphasis is placed on reducing compartments that strongly influence $\mathcal{R}_0$, while the quadratic cost term ensures a realistic balance between epidemiological benefit and implementation cost.

The admissible control set is defined by

$$U = \{u(t) \mid 0 \leq u(t) \leq 1\}.$$

The optimal control problem consists of finding $u^*(t) \in U$ such that

$$J(u^*) = \min_{u \in U} J(u).$$

To solve this problem, Pontryagin's Minimum Principle is applied. The Hamiltonian associated with system (21) is given by

$$\mathcal{H} = w_1 E + w_2 A + w_3 I + \frac{1}{2} w_4 u^2 + \sum_{i=1}^{6} \delta_i f_i,$$

where $\delta_i(t)$, $i = 1, \ldots, 6$, are the adjoint variables and f_i denote the right-hand sides of the state equations.

Theorem 5. *Let $u^*(t)$ be an optimal control with corresponding state trajectories $(S^*, E^*, A^*, I^*, H^*, R^*)$. Then there exist adjoint variables $\delta_i(t)$ satisfying the adjoint system*

$$\begin{aligned}
\dot{\delta}_1 &= \beta I \delta_1 + \mu\delta_1 + \epsilon u \delta_1 - \beta I \delta_2 - \epsilon u \delta_6,\\
\dot{\delta}_2 &= -w_1 + \delta_2(\mu + \alpha) - \delta_3 \alpha(1-p),\\
\dot{\delta}_3 &= -w_2 + \delta_3(\sigma + \psi + \mu) - \delta_4 \sigma - \delta_6 \psi,\\
\dot{\delta}_4 &= -w_3 - \beta S(\delta_1 + \delta_2) + \delta_4(\mu + \delta + \phi + \tau) - \delta_5 \phi - \delta_6 \tau,\\
\dot{\delta}_5 &= \delta_5(\mu + \delta + \gamma) - \delta_6 \gamma,\\
\dot{\delta}_6 &= -\nu\delta_1 + (\mu + \nu)\delta_6,
\end{aligned}$$

with transversality conditions $\delta_i(t_f) = 0$, $i = 1, \ldots, 6$. The optimal control is given by

$$u^*(t) = \min\left\{\max\left\{\frac{(\delta_1 - \delta_6)\epsilon S}{w_4}, 0\right\}, 1\right\}.$$

Proof. The result follows directly from Pontryagin's Minimum Principle [16]. The adjoint equations are obtained by differentiating the Hamiltonian with respect to the state variables, while the optimality condition is derived from $\partial\mathcal{H}/\partial u = 0$, yields

$$\frac{\partial \mathcal{H}}{\partial u} = 0 \iff u = \frac{(\delta_1 - \delta_6)\epsilon S}{w_4}.$$

Since it is defined that $0 \le u \le 1$, we obtain that $u^*(t)$ is

$$u^*(t) = \begin{cases} 0 & , \dfrac{(\delta_1 - \delta_6)\epsilon S}{w_4} \le 0 \\ \dfrac{(\delta_1 - \delta_6)\epsilon S}{w_4} & , 0 < \dfrac{(\delta_1 - \delta_6)\epsilon S}{w_4} < 1 \\ 1 & , \dfrac{(\delta_1 - \delta_6)\epsilon S}{w_4} \ge 1. \end{cases}$$

The optimal control function u can be written as follows:

$$u^*(t) = \min\left\{\max\left\{\frac{(\delta_1 - \delta_6)\epsilon S}{w_4}, 0\right\}, 1\right\}.$$

The convexity of the Hamiltonian in u, ensured by $\partial^2\mathcal{H}/\partial u^2 = w_4 > 0$, guarantees that the obtained control minimizes the objective functional. □

3.2. Numerical Results

To complement the analytical and sensitivity analyses, numerical simulations of system (1) are carried out using the baseline parameter values reported in Table 3. All simulations are implemented in Google Colab and are designed to serve two purposes: first, to illustrate the

long-term dynamical behavior of the model under varying reinfection scenarios; and second, to quantify the effectiveness of the optimal vaccination strategy. Together, the numerical results provide concrete evidence of how reinfection sustains endemic transmission and how targeted vaccination control suppresses epidemic burden across all compartments.

Table 3: Baseline values and ranges for parameters of Model (1)

Parameter	Baseline(range)	Units	Sources
Λ	73.648	person	[4]
μ	$3,5 \times 10^{-4}$	week^{-1}	[4]
δ	$3,286 \times 10^{-3}$	week^{-1}	[5]
β	$1,06 \times 10^{-9}$	week^{-1}	[5]
α	$1,674 \times 10^{-2}$	week^{-1}	[5]
p	4×10^{-1}	week^{-1}	[4]
σ	$7,218 \times 10^{-2}$	week^{-1}	[4]
ψ	$8,020 \times 10^{-3}$	week^{-1}	[4]
ϕ	5×10^{-1}	week^{-1}	[5]
τ	$8,836 \times 10^{-3}$	week^{-1}	[4]
γ	$3,6246 \times 10^{-2}$	week^{-1}	[5]
ν	7×10^{-3}	week^{-1}	estimated
ϵ	0,85	-	[4]

3.2.1. Effect of Reinfection on Disease Persistence

To isolate the role of reinfection in shaping the long-term transmission dynamics, numerical simulations are performed under two contrasting scenarios: the absence of reinfection ($\nu = 0$) and the presence of a small but positive reinfection rate ($\nu > 0$). The results are presented in Fig. 2.

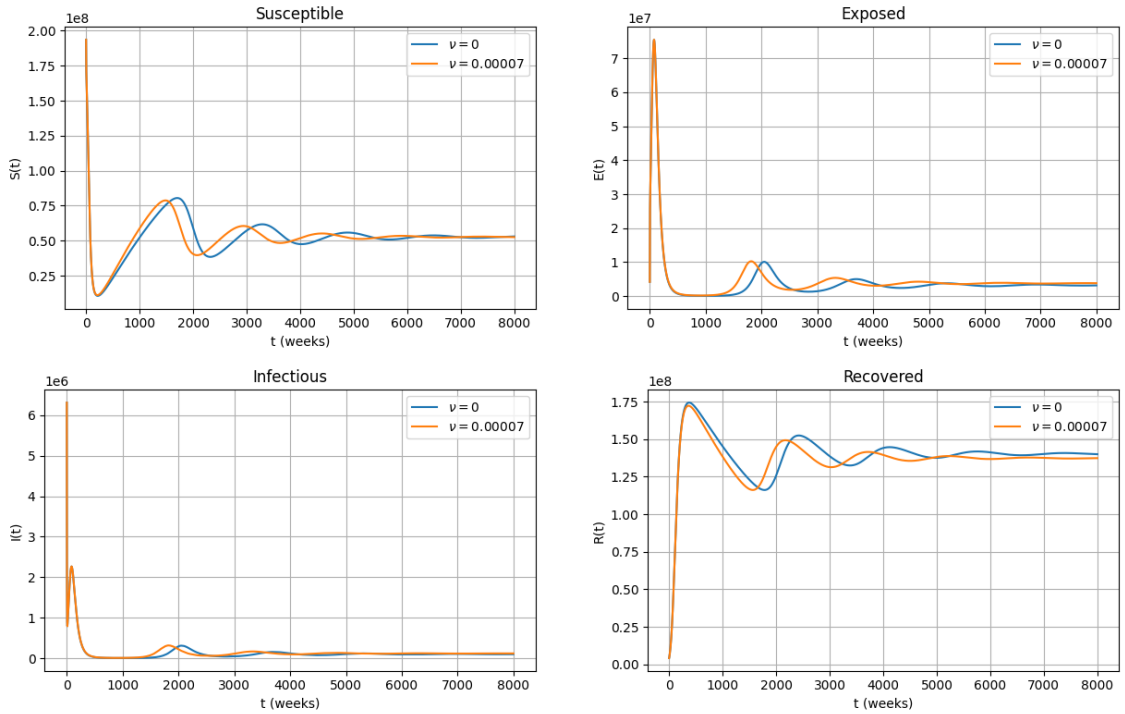

Fig. 2: Time evolution of selected subpopulations with and without reinfection

In the absence of reinfection ($\nu = 0$), the recovered compartment accumulates monotonically as individuals acquire permanent post-infection immunity, and the susceptible population is

progressively depleted without replenishment. Consequently, the force of infection diminishes over time, and both the exposed and symptomatic compartments decline steadily toward zero, indicating eventual disease elimination. This behavior is consistent with the classical threshold result: when the susceptible pool is sufficiently depleted, sustained transmission can no longer be maintained.

When a small reinfection rate is introduced ($\nu > 0$), however, the dynamic change qualitatively. Recovered individuals progressively return to the susceptible class as immunity wanes, continuously replenishing the pool of individuals available for new infection. This feedback mechanism sustains a non zero force of infection over the long term, preventing the decline of the exposed and infectious compartments to zero. Instead, both compartments converge to strictly positive steady states, and the system approaches an endemic equilibrium rather than disease-free elimination. The recovered population stabilizes at a slightly lower level compared to the $\nu = 0$ scenario, reflecting the ongoing outflow of individuals back to the susceptible class. These results demonstrate that even a numerically small reinfection rate can qualitatively alter the long-term behavior of the system — shifting the outcome from elimination to endemic persistence — consistent with the analytical condition established in Theorem 2. Notably, this transition occurs despite $\mathcal{R}_0$ remaining unchanged, since ν does not appear in the expression for $\mathcal{R}_0$; rather, reinfection acts through a distinct mechanism that replenishes susceptibility without affecting the initial invasion threshold.

3.2.2. Vaccine Control Simulation

The effectiveness of the optimal vaccination strategy derived in Section 3.1.8 is evaluated by comparing the trajectory of each compartment under two conditions: without control $u(t) = 0$ and with optimal vaccination control $u^*(t)$. The results are illustrated in Fig. 3 and summarized numerically in Table 4.

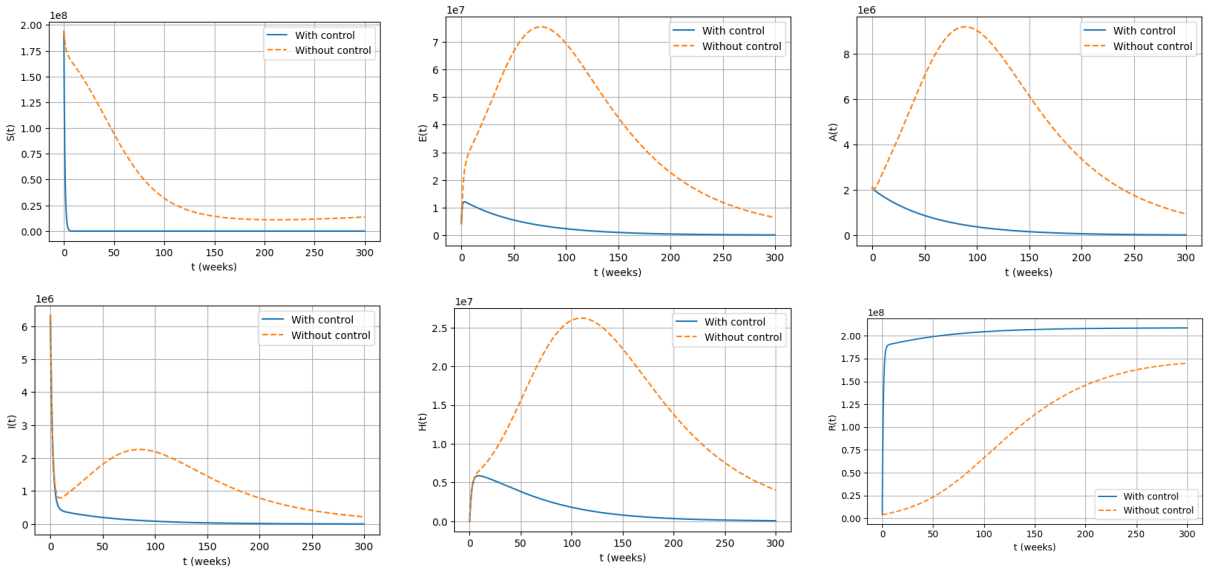

Fig. 3: Plot of each subpopulation before and after given vaccine control

Without vaccination control, the exposed (E), asymptomatic (A), and symptomatic (I) compartments remain elevated and do not decline toward zero within the simulation horizon, consistent with the analytical condition $\mathcal{R}_0 > 1$ under the baseline parameters. The susceptible population decreases gradually as individuals move into the exposed class, while the isolated compartment H accumulates reflecting uncontrolled case progression.

Under the optimal vaccination strategy, the dynamics are substantially altered. The susceptible population $S(t)$ declines rapidly in the early phase of the simulation due to intensive vaccination effort, as a large proportion of susceptible individuals are immunized and trans-

Table 4: Number of individuals in each subpopulation at baseline, without control, and with control

Subpopulation	**Initial Condition** $t = 0$	**Without control** $t = 100$	**With control** u $t = 100$
Susceptible	193.589.028	31.958.876	103.274
Exposed	4.208.457	69.428.305	2.518.506
Asymptomatic	2.104.228	9.008.299	398.308
Symptomatic	6.312.685	2.193.182	92.069
Isolated	0	25.925.040	1.918.127
Recovered	4.208.457	66.284.511	204.011.145
Total	210.422.855	204.798.213	209.041.429

Note: unit t in week

ferred to the recovered class. Correspondingly, the exposed, asymptomatic, and symptomatic compartments exhibit markedly accelerated declines compared to the uncontrolled scenario. In particular, the symptomatic class $I(t)$ approaches near-zero levels within a considerably shorter time horizon, reflecting the direct reduction in susceptibility and the consequent suppression of the force of infection. The isolated compartment $H(t)$ exhibits a transient increase in the early period of control implementation, attributable to enhanced detection and referral of existing cases, before declining steadily as the upstream infectious compartments are brought under control. Meanwhile, the recovered population $R(t)$ rises markedly under vaccination, reflecting immunity acquisition through both natural recovery and successful immunization.

These dynamics are further quantified in Table 4. At $t = 100$ weeks, the number of symptomatic individuals under control is reduced to 92,069 compared to 2,193,182 in the uncontrolled scenario — a reduction of approximately 95.8%. The exposed and asymptomatic compartments exhibit reductions of approximately 96.4% and 95.6%, respectively, while the recovered population increases from 66,284,511 to 204,011,145, confirming large-scale immunity acquisition under the vaccination strategy.

The following plot shows the cost function when vaccination control u is implemented. The

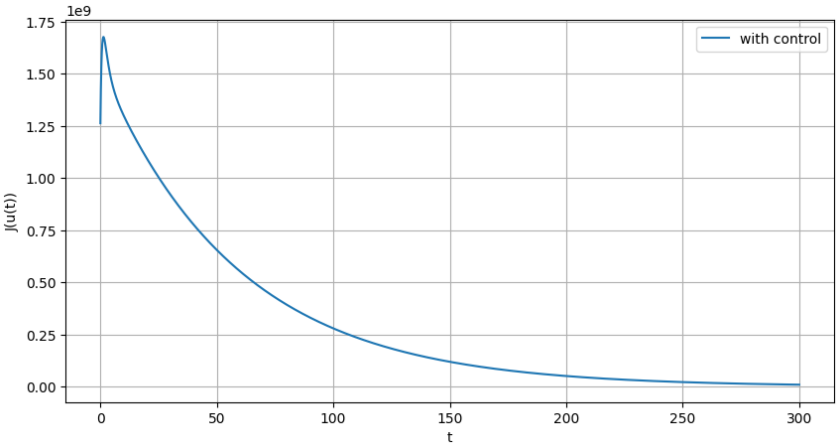

Fig. 4: Plot of the cost when vaccination control is given u

temporal profile of the cost functional $J(u)$ is presented in Fig. 4. The cost is highest in the early phase of the simulation, when infection levels are large and vaccination effort must be intensive to bring the epidemic under control. As the infected compartments decline, the cost functional decreases rapidly and approaches zero toward the end of the simulation horizon, indicating that the optimal strategy efficiently redistributes vaccination effort over time rather than sustaining maximal effort indefinitely. This behavior reflects the structure of the quadratic cost term in the objective functional, which penalizes excessive vaccination intensity and naturally encourages a front-loaded but self-regulating control profile.

4. Conclusion

This study developed and analyzed a deterministic $SEAIHR$ compartment model describing mpox transmission dynamics with waning immunity and reinfection. The model admits a disease-free equilibrium $\mathcal{E}_0 = (\Lambda/\mu, 0, 0, 0, 0, 0)$ and a unique endemic equilibrium given in Eq. (9). Rigorous stability analysis established that the disease-free equilibrium is both locally and globally asymptotically stable when $\mathcal{R}_0 < 1$, guaranteeing disease elimination under sufficiently controlled transmission, while the endemic equilibrium is conditionally globally asymptotically stable when $\mathcal{R}_0 > 1$ under the sufficient conditions stated in Proposition 1. These threshold results provide a mathematically precise basis for evaluating the long-term epidemiological consequences of intervention strategies.

Sensitivity analysis of $\mathcal{R}_0$ revealed that the transmission rate β and the isolation rate ϕ are the most influential parameters governing infection risk and control, respectively. In particular, β carries a unit sensitivity index, underscoring that any reduction in effective contact, whether through behavioral change or vaccination, produces a proportionally equivalent reduction in $\mathcal{R}_0$. Conversely, ϕ exhibits the strongest negative sensitivity, confirming that rapid identification and isolation of symptomatic individuals constitutes the most operationally direct mechanism for suppressing transmission at the community level.

Motivated by these findings, an optimal control framework was formulated in which vaccination is incorporated as a time-dependent control variable applied to the susceptible population. The optimal strategy was explicitly characterized using Pontryagin's Minimum Principle, yielding a closed-form expression for $u^*(t)$ that dynamically balances epidemiological benefit against implementation cost. Numerical simulations confirmed the theoretical results and demonstrated that optimal vaccination substantially reduces the exposed, asymptomatic, and symptomatic compartments, achieving reductions of approximately $96.4\%, 95.6\%, and 95.8\%$, respectively, at $t = 100$ weeks relative to the uncontrolled scenario. Furthermore, the cost functional profile shows that the optimal strategy is front-loaded in its vaccination intensity, self-regulating as infection levels decline, which reflects a realistic and resource-efficient deployment profile.

The inclusion of reinfection via waning immunity reveals an important dynamical feature that is absent from classical permanent-immunity models: even a numerically small reinfection rate ν can qualitatively shift the long-term behavior of the system from disease elimination to endemic persistence, without altering $\mathcal{R}_0$ itself. This finding has direct public health implications, suggesting that epidemic models that neglect waning immunity may systematically underestimate the risk of long-term endemic establishment, particularly in settings where booster vaccination is unavailable or delayed.

The proposed model, however, carries several limitations that should be acknowledged. First, zoonotic transmission from animal reservoirs is not incorporated, so the model is most appropriate for analyzing sustained human-to-human transmission at the community level rather than spillover-driven dynamics. Second, asymptomatic individuals are assumed non-infectious, which may underestimate transmission in settings where pre-symptomatic spread occurs. Third, homogeneous mixing is assumed throughout, precluding the effects of age structure, contact heterogeneity, and behavioral risk factors. Fourth, the mass-action incidence formulation implies that transmission scales with absolute population size, which may not be realistic in large or spatially dispersed populations where frequency-dependent contact patterns are more appropriate. Finally, both immunity waning and reinfection are captured by constant rates, which represents a simplification of the complex and time-varying immunological processes governing post-infection and post-vaccination protection.

These limitations delineate clear directions for future work. Model extensions incorporating age-structured contact matrices, frequency-dependent incidence, stochastic transmission, waning vaccine-induced immunity as a separate compartmental process, and data-driven parameter estimation from recent mpox outbreak records would substantially enhance the epidemiological realism and predictive capacity of the framework developed here.

CRediT Authorship Contribution Statement

Eka Widia Rahayu: Conceptualization, Methodology, Writing–Original Draft, Data Curation, Formal Analysis. **Noorma Yulia Megawati:** Validation, Writing–Review & Editing.

Declaration of Generative AI and AI-assisted technologies

In the preparation of this manuscript, the authors used ChatGPT (OpenAI) and Grammarly for writing assistance, proofreading and language editing. These tools were used solely to improve the readability and grammatical accuracy of the manuscript. The authors have reviewed and take full responsibility for the content of the publication.

Declaration of Competing Interest

The authors declare no competing interests

Funding and Acknowledgments

The authors declare that no financial support was received for the research, authorship, or publication of this article.

Data and Code Availability

The data and code supporting the findings of this study are available from the corresponding author upon reasonable request and subject to confidentiality agreements.

References

[1] Centers for Disease Control and Prevention. *Mpox*. 2025. https://www.cdc.gov/mpox/about/index.html.

[2] Kementerian Kesehatan Republik Indonesia. *Monkeypox: Frequently Asked Questions (FAQ)*. Kementerian Kesehatan RI. Jakarta, 2022. https://share.google/PTASQG00aIol31BBV.

[3] Dimie Ogoina, Inger Damon, and Etienne Nakoune. "Clinical review of human mpox". In: *Clinical Microbiology and Infection* 29.11 (2023), pp. 1493–1501. DOI: 10.1016/j.cmi.2023.09.006.

[4] Y. U. Ahmad, J. Andrawus, A. Ado, Y. A. Maigoro, A. Yusuf, S. Althobaiti, and U. T. Mustapha. "Mathematical modeling and analysis of human-to-human monkeypox virus transmission with post-exposure vaccination". In: *Modeling Earth Systems and Environment* 10 (2024), pp. 2711–2731. DOI: 10.1007/s40808-023-01920-1.

[5] O. J. Peter, S. Kumar, N. Kumari, F. A. Oguntolu, K. Oshinubi, and R. Musa. "Transmission dynamics of Monkeypox virus: a mathematical modelling approach". In: *Modeling Earth Systems and Environment* (2022), pp. 1–12. DOI: 10.1007/s40808-021-01313-2.

[6] S. Usman and I. I. Adamu. "Modeling the Transmission Dynamics of the Monkeypox Virus Infection with Treatment and Vaccination Interventions". In: *Journal of Applied Mathematics and Physics* (2017), pp. 2335–2353. DOI: 10.4236/jamp.2017.512191.

[7] Lawrence Perko. *Differential Equations and Dynamical Systems*. 3rd ed. New York: Springer, 2001. DOI: 10.1007/978-1-4613-0003-8.

[8] Stephen Wiggins. *Introduction to Applied Nonlinear Dynamical Systems and Chaos*. 2nd ed. New York: Springer-Verlag, 2003. DOI: 10.1007/b97481.

[9] Wassim M. Haddad, VijaySekhar Chellaboina, and Qing Hui. *Nonnegative and Compartmental Dynamical Systems*. Princeton: Princeton University Press, 2010. DOI: 10.1515/9781400832248.

[10] Fred Brauer and Carlos Chaves. *Mathematical Models in Population Biology and Epidemiology*. 2nd ed. New York: Springer, 2012. DOI: 10.1007/978-1-4614-1686-9.

[11] Pauline Van den Driessche and James Watmough. "Reproduction number and sub-threshold endemic equilibria for compartmental models of disease transmission". In: *Mathematical Biosciences* 180 (2002), pp. 29–48. DOI: 10.1016/s0025-5564(02)00108-6.

[12] O. Diekmann and J. A. P. Heesterbeek. "On the definition and the computation of the basic reproduction ratio $\mathcal{R}_0$ in models for infectious diseases in heterogeneous populations". In: *Journal of Mathematical Biology* 28 (1990), pp. 365–382. DOI: 10.1007/BF00178324.

[13] Maia Martcheva. *An Introduction to Mathematical Epidemiology*. New York: Springer, 2015. DOI: 10.1007/978-1-4899-7612-3..

[14] Stephen Boyd. *Basic Lyapunov Theory*. Stanford: Stanford University, 2008. https://web.stanford.edu/class/ee363/lectures/lyap.pdf.

[15] Nakul Chitnis, James M. Hyman, and Jim M. Cushing. "Determining important parameters in the spread of malaria through the sensitivity analysis of a mathematical model". In: *Bulletin of Mathematical Biology* 70.5 (2008), pp. 1272–1296. DOI: 10.1007/s11538-008-9299-0.

[16] D. Subbaram Naidu. *Optimal Control Systems*. New York: CRC Press, 2002. http://103.203.175.90:81/fdScript/RootOfEBooks/E%20Book%20collection%20-%202026%20-%20F/EEE/optimal%20control%20systems,subbaram%20naidu.pdf.